

UNCLASSIFIED

AD NUMBER
AD894251
NEW LIMITATION CHANGE
TO Approved for public release, distribution unlimited
FROM Distribution authorized to U.S. Gov't. agencies only; Test and Evaluation; 15 FEB 1972. Other requests shall be referred to the Naval Air Systems Command, Washington, DC 20360.
AUTHORITY
USNWC ltr, dtd 30 AUG 1974

THIS PAGE IS UNCLASSIFIED



AD 894251

FILE COPY

Beam Uniformity Measurements for Q-Switched Nd:YAG Lasers

by
Edward A. Teppo
Weapons Development Department

DDC
RECEIVED
MAY 19 1972
RECEIVED

Naval Weapons Center

CHINA LAKE, CALIFORNIA ■ FEBRUARY 1972



33

ABSTRACT

The output beam uniformity of a Q-switched Nd:YAG laser, using four different flashlamp-laser rod pump cavity coupling configurations, is described. The test apparatus and test procedure used to establish the beam uniformity quantitatively are given.

A newly defined beam uniformity parameter M^* , the ratio of maximum-to-average peak power density, is shown to vary significantly for the pump cavities tested. The data presented on beam uniformity is applicable toward improving laser pump cavity design, interpreting particular missile and seeker tracking behavior, comparing techniques for measuring laser beam divergence and is an aid in establishing the damage threshold level for retinal tissues and laser resonator components at 1.06μ .

ACCESSION for	
CFSTI	WHITE SECTION <input type="checkbox"/>
DOC	BLUE SECTION <input checked="" type="checkbox"/>
UNANNOUNCED	<input type="checkbox"/>
JUSTIFICATION	
.....	
BY	
DISTRIBUTION/AVAILABILITY CODES	
DIST.	AVAIL. AND/OR SPECIAL
B	

NWC Technical Publication 5315

Published by Weapons Development Department
 Manuscript 40/MS 72-5
 Collation Cover, 15 leaves, DD Form 1473, abstract cards
 First printing 135 unnumbered copies
 Security classification UNCLASSIFIED

Naval Weapons Center

AN ACTIVITY OF THE NAVAL MATERIAL COMMAND

W. J. Moran, RADM, USN Commander

H. G. Wilson Technical Director

FOREWORD

Beam uniformity measurements for a Q-switched Nd:YAG laser are described. A beam uniformity parameter M^* is defined and then measured experimentally for several flashlamp-laser rod pump cavity configurations. The parameter M^* (pronounced "M-Star") is shown to be an important quantity in many applications, including particular missile and seeker guidance, laser safety, and intra-resonator component damage phenomenon.

The investigation was undertaken after it was learned that particular Nd:YAG lasers having similar energy output and beam divergence perform differently in the system application. This study showed that the beam uniformity and the parameter M^* , which describes uniformity quantitatively, can be used to interpret some of the operational characteristics of the Q-switched Nd:YAG laser. The study was performed during the period September-November 1971 and was done under Weapons Development Department laser technology funding.

This publication is released at the working level for information only.

Released by
C. P. SMITH, *Head*
Infrared Systems Division
11 January 1972

Under authority of
F. H. KNEMEYER, *Head*
Weapons Development Department

CONTENTS

Introduction	1
The M* Parameter	2
Test Apparatus	4
Test Procedure	7
Results and Discussion	9
Beam Uniformity Near the Resonator	9
Energy Output Stability	17
Hot Spot Sizing	17
Far Field Beam Uniformity	20
Beam Divergence Measurements	21
Lasing Area and an M* Data Summary	24
Conclusion	27

ACKNOWLEDGMENT

The author wishes to acknowledge the support of T. Wae of the Laser Controls Branch (Code 4057), Weapons Development Department, who designed the sample-and-hold circuit.

INTRODUCTION

The solid-state Nd:YAG laser has found widespread use in both industrial and military applications. Its improved thermal properties and operating efficiency--as compared to Nd:glass and ruby--are its major attributes and allow its use in both the pulsed and continuous-wave mode of operation. Two of the most important output properties of a Q-switched Nd:YAG laser, regardless of its application, are its peak power and beam divergence.

The peak power is usually determined by establishing the ratio of laser output energy to output pulse width, each quantity being measured separately. The beam divergence is usually determined by establishing the size of an aperture in a positive lens focal plane required to pass 90% of the laser output energy. Unfortunately, all of these measurements are relatively insensitive to the beam uniformity properties of the laser output.

This output beam uniformity is important to evaluate for several reasons. Beam uniformity data can be used to improve laser pump cavity design by selecting or designing pump cavities that pump the laser rod as uniformly as possible. "Hot spots" in laser beams should be quantitatively interpreted and their effect on laser beam spot tracker performance determined. These "hot spots" are important to evaluate from the laser safety standpoint as well, both in establishing safe exposure levels for particular 1.06- μ lasers and as an aid in establishing the actual energy density damage threshold level for retinal tissues. Some laser resonators are limited in output peak power due to surface damage effects on intra-resonator components and so the beam uniformity is important in these cases as well.

The measurement of output beam uniformity in the focal plane of a converging lens has at least three important purposes:

1. This far field peak power density distribution is analogous to that found at a laser-designated target assuming no atmospheric effects significantly alter the beam distribution between the laser and the target. Most atmospheric effects are expected to modify the beam distribution randomly from point-to-point over the beam size. Thus the beam distribution would not be altered in a way that is dependent upon the beam peak power density at any point in the beam. Particular missile and seeker tracking systems are inherently aware of this quantitative

beam uniformity, especially if the receiver employs centroid tracking characteristics. It is important then that the beam uniformity parameter M^* be examined to help understand its effect on tracking behavior for target acquisition systems and terminal guidance characteristics of particular missiles. The beam uniformity for lasers used in flight simulators for such systems should also be determined.

2. The quantitative far field beam uniformity is an aid in establishing laser safety criteria for field and lab usage of Q-switched Nd:YAG lasers. The beam uniformity, being different for various lasers, is also important in establishing the absolute threshold energy density for laser damage to retinal tissues at 1.06μ . It has been found that lasers having the same output energy and beam divergence can yield different eye damage threshold level results. The beam uniformity parameter M^* , being different for various coupling configurations, would contribute to such an effect.

3. Since laser beam divergence is generally measured in the focal plane of a positive lens, techniques for measuring this important laser output parameter can be compared by evaluation of the far field peak power density distribution. Data will be presented here showing the widely different far field beam uniformity profiles for a diffusely reflecting and silvered close-wrapped pump cavity configuration.

The laser output beam uniformity has been examined in detail both near the resonator output aperture and in the focal plane of a positive lens. The output beam uniformity will be shown to vary considerably for the several flashlamp-laser rod coupling configurations tested. A newly defined beam uniformity parameter M^* (pronounced "M-Star") will be shown to be an important parameter in many applications of Q-switched Nd:YAG lasers.

THE M^* PARAMETER

The peak power in megawatts (MW) of a Q-switched laser is given by the ratio of output energy E (in millijoules) to output pulse width T (in nanoseconds). For example, a laser with a 100-mJ output energy and a 10-nsec pulse width has an output peak power of 10 MW. The peak power density P_o in MW/cm^2 is then this peak power distributed over the lasing area A (in cm^2) and can be expressed directly as

$$P_o = E/TA \quad \text{in MW/cm}^2 \quad (1)$$

This result inherently assumes that the output energy E is uniform over the laser beam area A , i.e., that the output beam is uniform. The maximum peak power density P_m is here defined as

$$P_m = M^* P_o = M^* E/TA \quad \text{in MW/cm}^2 \quad (2)$$

where M^* is the ratio of the maximum peak power density (PPD) to the (average) PPD described by Eq. 1. Beam uniformity will be described in terms of this experimentally determined parameter M^* . Note that, if the output beam is absolutely uniform, then $M^* = 1.0$ and a measurement of energy density anywhere within the output laser beam is a constant. However, Nd:YAG lasers having very similar output energy and beam divergence figure may have appreciably different values of M^* (and hence appreciably different values of maximum peak power density as well).

The maximum PPD of a pulse from a laser resonator, defined in Eq. 2, is directly proportional to the maximum PPD within the laser resonator (P'_m). For a resonator using a partially transmitting end mirror of reflectivity R , it can be shown that

$$\begin{aligned} P'_m &= P_m (1 + R)/(1 - R) && \text{in MW/cm}^2 \\ &= M^* E/TA \cdot (1 + R)/(1 - R) \end{aligned} \quad (3)$$

Within the resonator, the maximum PPD is particularly of interest if a lithium niobate crystal is used as the Q-switch element. This Q-switch is readily damaged by high PPD radiation, and a pump cavity design that provides the highest possible intra-resonator beam uniformity as well as a high flashlamp-laser rod coupling efficiency is desirable.

The beam uniformity within the resonator is dependent upon the mode structure. From resonator theory it can be shown that the lowest order Gaussian mode for a typical Q-switched Nd:YAG laser resonator has a diameter of approximately 0.5 mm. Unfortunately the cross-sectional area of the resonator (typically about 0.3 cm^2) is much larger than the cross-sectional area of a single mode. This means that the resonator Fresnel number is large and energy from many transverse modes is contributed simultaneously to the laser output. The peak amplitudes of several transverse modes may overlap in small regions of the laser rod cross section and the resultant PPD in these areas is represented by a complex superposition of the PPDs of the individual modes present. This superposition, in turn, increases the beam nonuniformity and so M^* increases. These higher order modes have larger diameters than the lowest order mode, and so such a superposition of modes in any area of the laser rod cross section should not produce "hot spots" much smaller than the lowest order mode diameter. The concept of "hot spots" is not new to laser resonators, but the size of "hot spots" in laser beams has not been studied in detail in the past.

The test apparatus and test procedure for making the M^* measurement, both near the resonator output aperture and in a lens focal plane, are described in the next section.

TEST APPARATUS

The test apparatus used to determine the beam uniformity parameter M^* is shown in Fig. 1. The in-line laser resonator was near 30 cm in optical path length. The flat end-dump output mirror was 50% reflective. Both flat and 10-meter radius of curvature, 100% reflecting end mirrors were used as the second laser reflector. The 9 x 9 x 10 mm lithium niobate modulator was driven electronically in such a way as to ensure that a single Q-switched laser output pulse occurred by using appropriate hold-off voltage, modulator voltage pulse amplitude and rise time, and trigger delay with respect to the flashlamp current pulse. The Glan air laser prism allowed the use of an in-line resonator configuration and provided ease in resonator alignment. The laser coolant was FC-104, the pulse repetition rate was 10 Hz and the pump energy was 8 joules per pulse. The output energy was typically 110 mJ and the output pulse width (FWHM) was approximately 15 nsec. The same 1/4- x 3-inch laser rod and 6 mm OD, 1,500 torr, krypton-filled flashlamp was used for all the tests performed.

The Q-switched laser output was attenuated by two flat, highly reflective, dielectrically coated, (laser) mirrors and a 0.001-inch diameter aperture (to be called the scan aperture) placed over an EG&G-SGD-040 planar-diffused silicon photodiode. The photodiode was placed either near the 50% reflective output end mirror of the laser resonator or in the focal plane of a positive lens. The high reflectivity attenuators were skewed to prevent multiple reflection effects at the photodiode. A large limiting aperture was used in front of the detector scan assembly. Extreme care was required and taken to prevent stray laser radiation from being detected. The laser radiation reflected from the first attenuator was used to monitor the energy output of the resonator and compare the output energy stability to the photodiode output stability at various positions of the scan aperture. The SGD-040 photodiode was mounted on an XY translational stage and was moved manually in an array whose elements were separated by 0.025 inch in rows and columns. This separation between data matrix elements seemed a reasonable compromise between beam uniformity resolution and laser run time needed to establish the matrix elements. A typical array of data points (which constitute the data matrix) is shown in Fig. 2. The approximate position of the laser rod with respect to the data matrix is shown and its precise position relative to the matrix elements was not required. For the far field measurements, the scan aperture was also moved in 0.025-inch increments in the focal plane of a 40.5-inch focal length lens which corresponded to increments of beam spread of $0.025 \text{ inch}/40.5 \text{ inches} = 0.617 \text{ mrad}$.

The photodiode output current pulse provided the input to the sample-and-hold circuit shown in Fig. 3. This circuit was basically energy-detecting where the voltage at the $\mu A740$ input was proportional to the charge accumulated on the 1,000-pF, low-loss, glass ceramic capacitor. The 1N3595 and FD700 diodes in series provided a combination

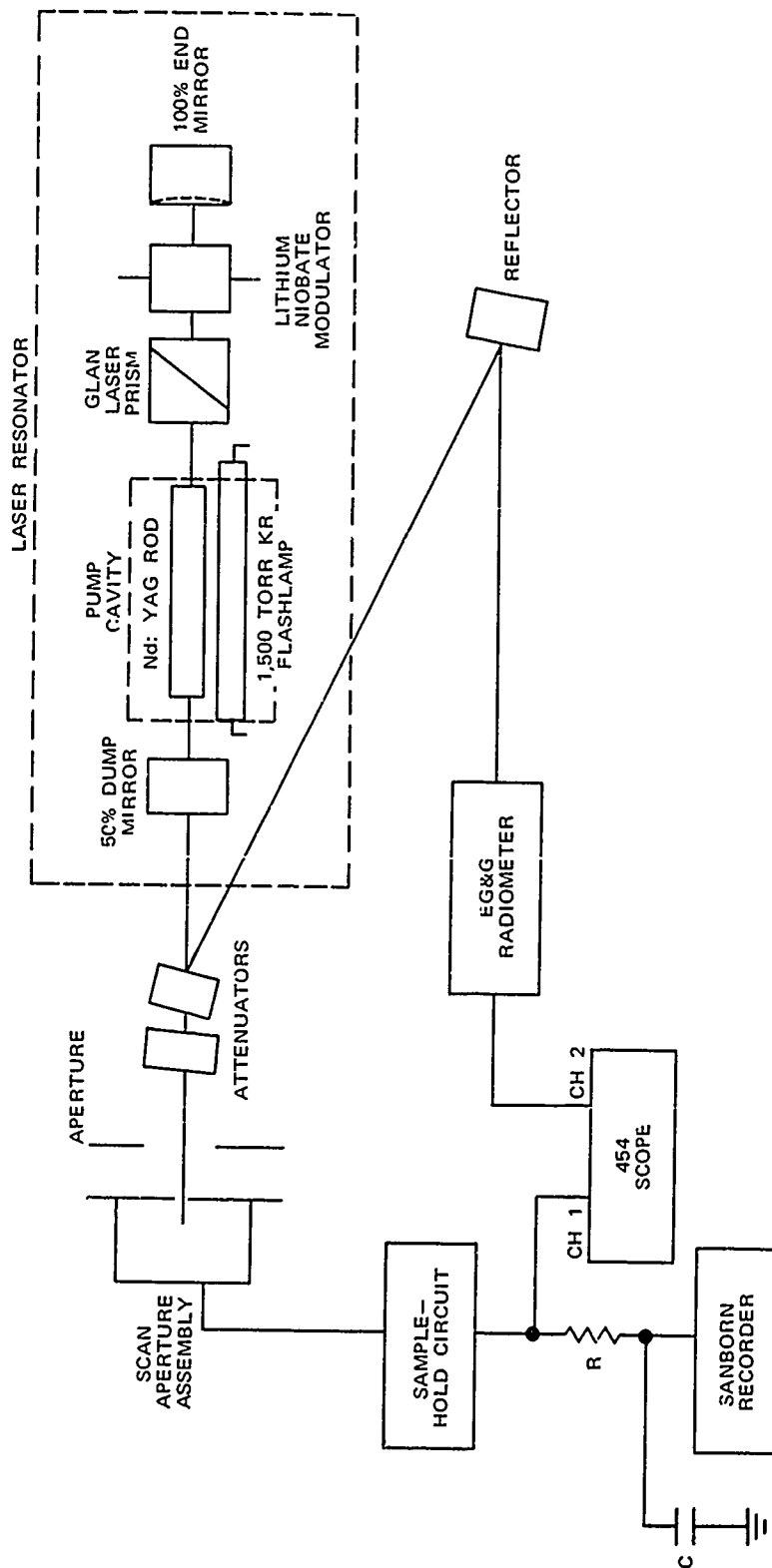


FIG. 1. Test Apparatus.

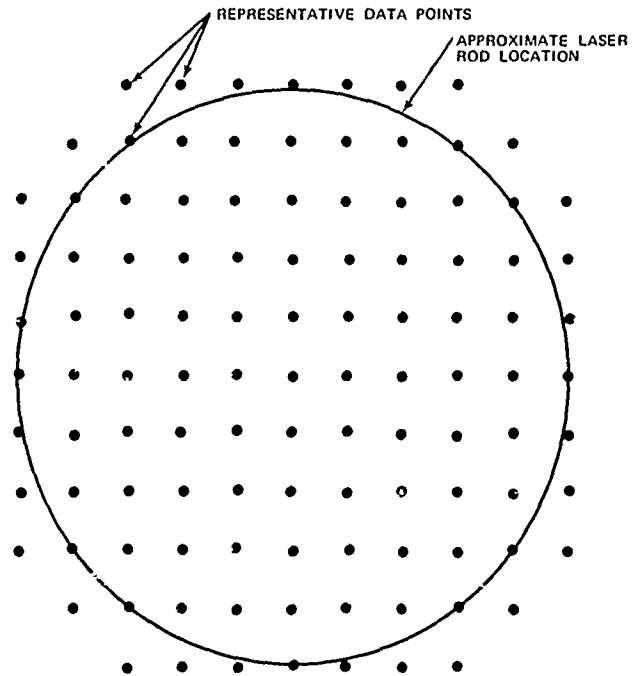


FIG. 2. Data Matrix for Peak Power Density Distribution.

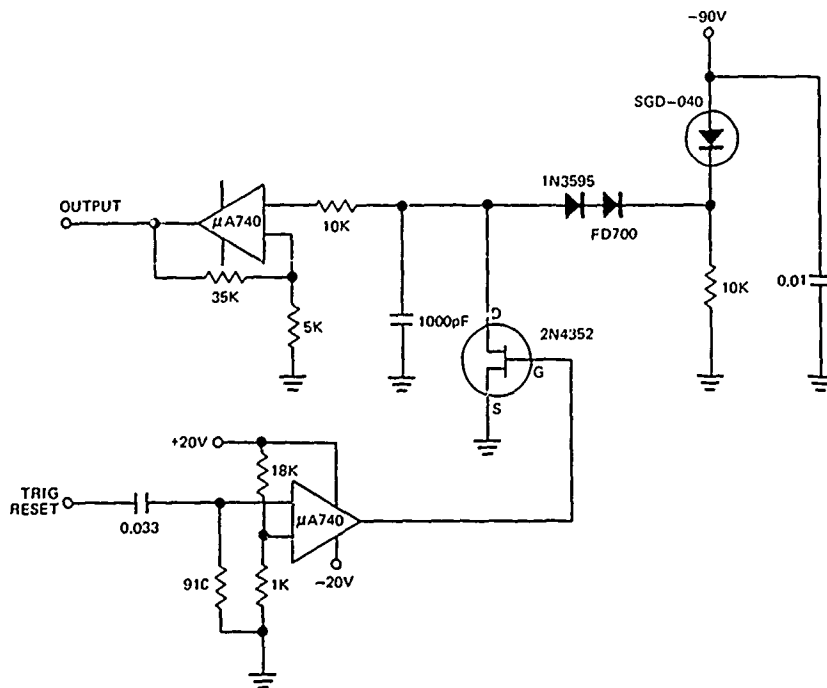


FIG. 3. Sample-and-Hold Circuit.

of low leakage and fast response to the detected laser energy. The flashlamp trigger pulse signal supplied the TRIG RESET function which caused the 2N4352 MOSFET to conduct and clear the charge from the 1,000-pF capacitor. The saturated signal output of the μ A740 was near -18 volts and the maximum operational signal level used was near -5 volts. The bias supply voltages for the μ A740s was carefully matched. Since the PPD is directly proportional to the (detected) energy for constant output pulse width (see Eq. 1), the μ A740 output voltage level was proportional to the PPD received at the SGD-040 photodiode. The μ A740 output voltage was nearly constant for 95 msec of any laser interpulse period of 100 msec (due to the 10 Hz repetition rate of the laser). The sample-and-hold circuit output was integrated by a 1-sec time constant at the input to a Sanborn strip chart recorder, which meant that approximately 10 laser output pulses were averaged. This time-averaging improved the recorder output stability slightly since the 5 msec that the μ A740 input was grounded per laser interpulse period went unnoticed at the μ A740 output.

TEST PROCEDURE

The test procedure involved moving the 0.001-inch diameter scan aperture in 0.025-inch increments in the horizontal plane with successive steps of 0.025 inch in the vertical plane until the signal voltage level at the data matrix element location became insignificant. The individual data matrix element signal level was proportional to the PPD at that matrix element position. Figure 4 shows the individual data matrix elements for a slightly misaligned laser resonator. The beam uniformity parameter M^* can be determined from this representative data matrix using two techniques: discrete point-averaging or area-averaging.

The discrete point-averaging method involves simply summing all recorded signal levels and dividing by the number of elements recorded. For the example case used in Fig. 4, it follows that $(0.5 + 0.8 + 0.7 + \dots + 30.0 + 30.0 + \dots + 1.2 + 0.8)/83 = 717.3/83 = 8.6$ is the average signal level recorded. Therefore, $M^* = 30.0/8.6 = 3.5$ for this case (using the discrete point-averaging technique), since M^* is experimentally the ratio of the peak-to-average signal level for all the data matrix elements. The area-averaging technique involves finding the average signal amplitude for areas 0.025 inch on a side. For example, the average amplitude of the area element A shown in Fig. 4 is given simply by $(0.5 + 0.8 + 4 + 6.5)/4 = 2.9$. So then, area-averaging involves summing all these area elements and dividing by their number. The discrete point-averaging technique provides a slightly larger M^* value as compared to the area-averaging technique since, in area-averaging, data matrix elements near the beam edge are weighted less than data matrix elements toward the laser rod center. The discrete point-averaging technique to determine M^* , besides being faster to compute, is also more representative for comparing an average PPD figure

to a (true point) PPD value. This discrete point-averaging technique to determine M^* was used exclusively in the description that follows.

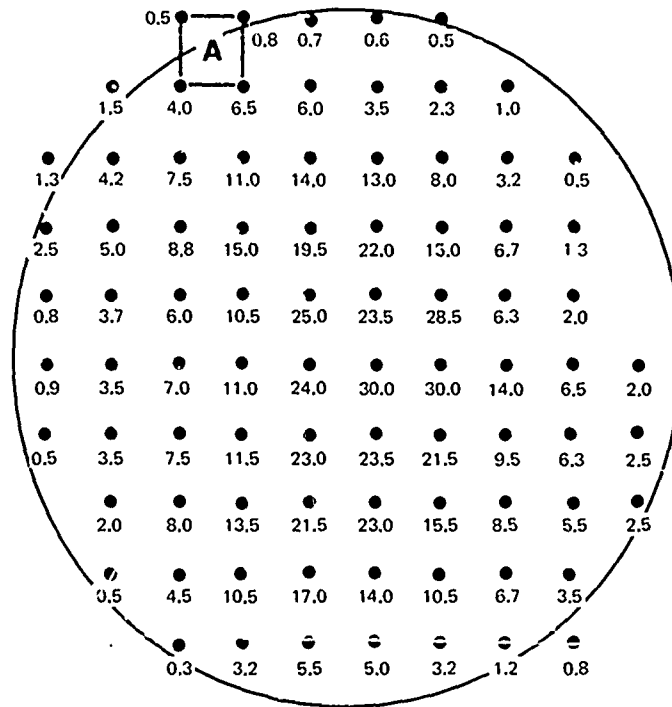


FIG. 4. Data Matrix Elements for a Misaligned Cylindrical Pump Cavity.

Contour lines of constant signal amplitude (or constant PPD) can be drawn on these data matrices as shown in Fig. 5. The contours shown correspond to signal levels of 2.5, 5, 10, 15, 20, 25, and 30 units. Suppose (for example) that the average signal level for this data matrix is 10 units. Then the "20-unit" contour line drawn represents a constant PPD twice as high as the average PPD and the "5-unit" contour line represents that position in the laser output having half the average PPD. The individual data matrix elements will not be shown on all the contour diagrams that follow and, for the most part, only the most intense signal level recorded and its position on the contour mapping will be shown.

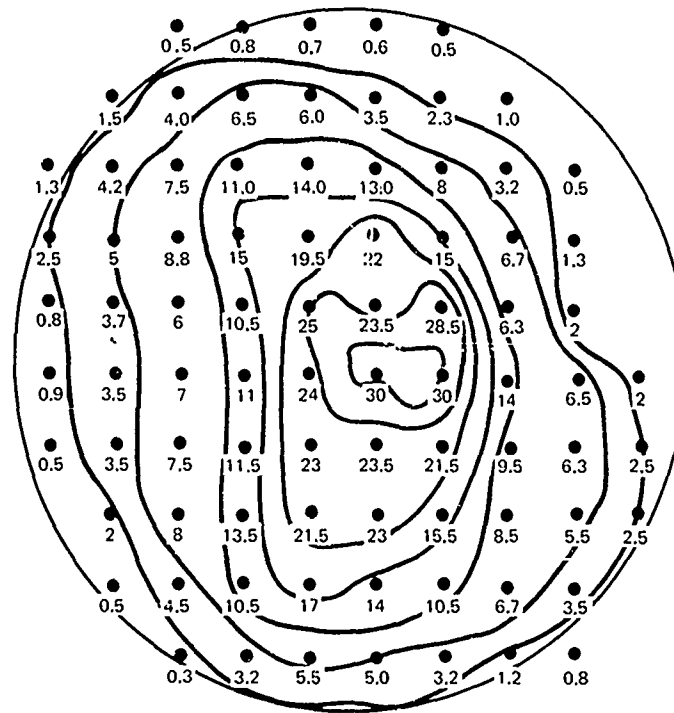


FIG. 5. Constant Peak Power Density Contour Mapping.

RESULTS AND DISCUSSION

BEAM UNIFORMITY NEAR THE RESONATOR

In all, four different flashlamp-laser rod coupling configurations were tested: silvered cylindrical, silvered cylindrical with inserts, diffuse cylindrical, and silvered close-wrapped. Approximate 8:5 scale drawings of the pump cavity shapes are shown in Fig. 6 with the flashlamp and laser rod enclosed. It should be made clear that the beam uniformity contours to be provided are unique to the pump cavities tested. It is more than likely that the beam uniformity contours and M^2 will change if the physical dimensions of the pump cavity change in any way.

Figure 7 shows representative PPD distribution contours for a silvered cylindrical pump cavity with inserts for both types of end mirrors used in conjunction with this coupling configuration. The M^2 figure using a flat end mirror was 3.75; with a 10-meter (radius of

curvature) end mirror used as the 100% end reflector, $M^* = 4.0$. (The output energy was nearly 10% lower when the flat end mirror was used.) These test results indicate that, for this silvered cylindrical pump cavity with inserts, the maximum PPD is nearly four times larger than the average PPD. The average M^* value measured for the cylindrical pump cavity with inserts was $M^* = 3.86$. Burn patterns on exposed Polaroid film showed an excellent qualitative correlation to the contour mapping profile within the resolution accuracy of the mapping made.

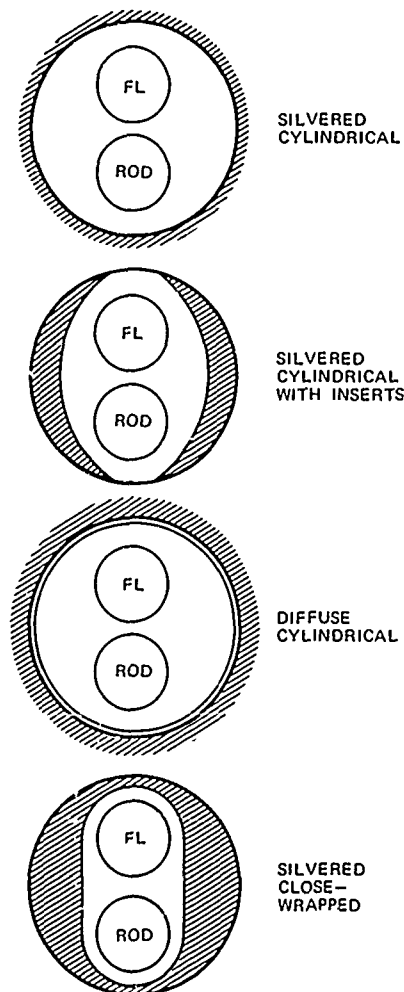
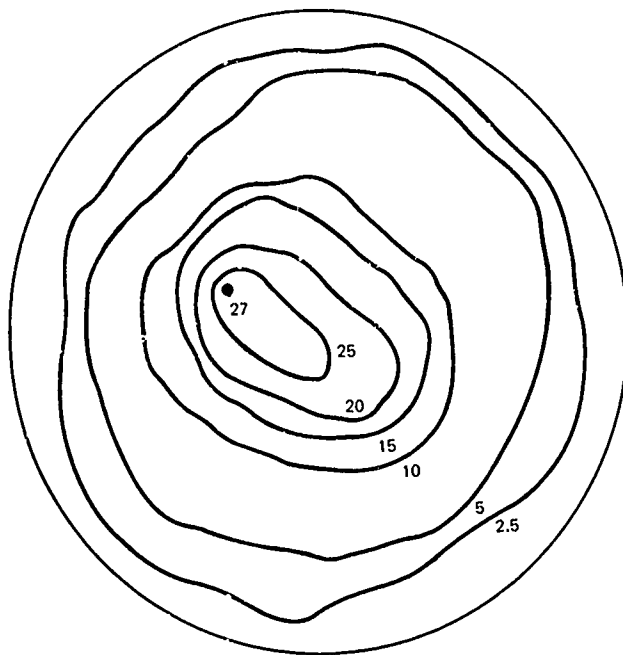
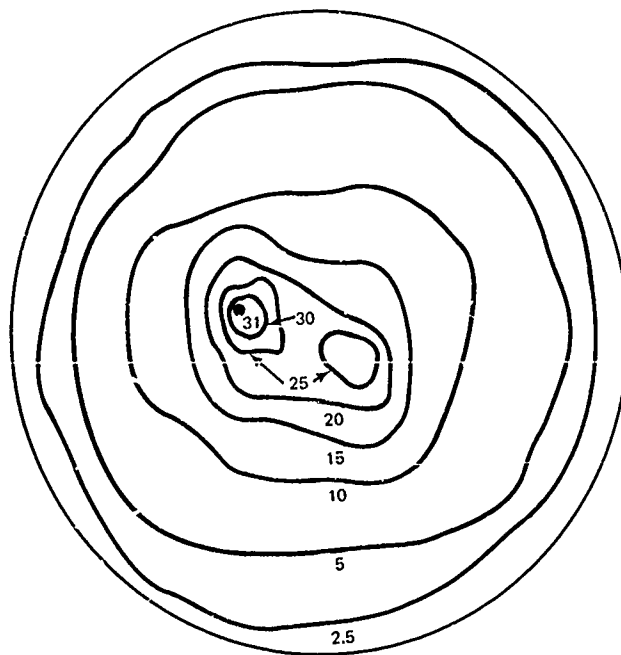


FIG. 6. Flashlamp-Laser Rod Coupling Configurations.



$M^* = 3.75$

(a) Flat end reflector.

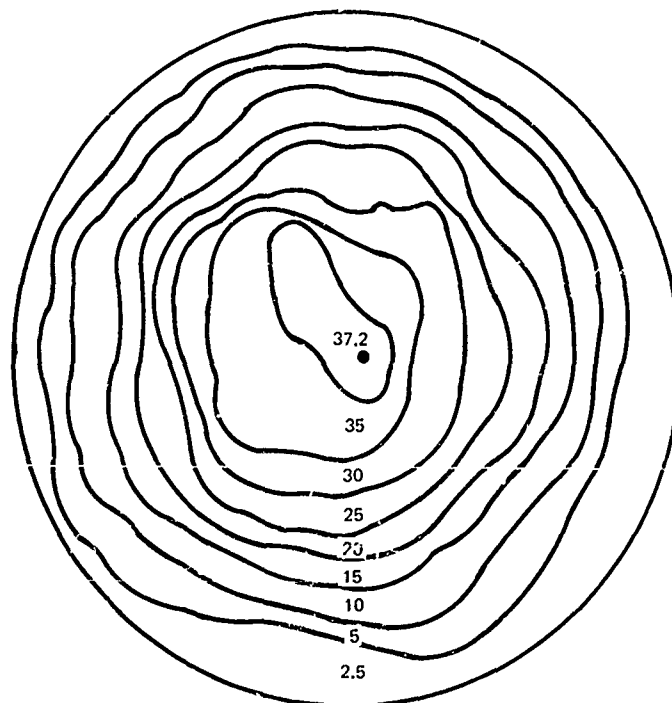


$M^* = 4.0$

(b) 10-m end reflector.

FIG. 7. Peak Power Density Distribution for a Cylindrical Pump Cavity With Inserts.

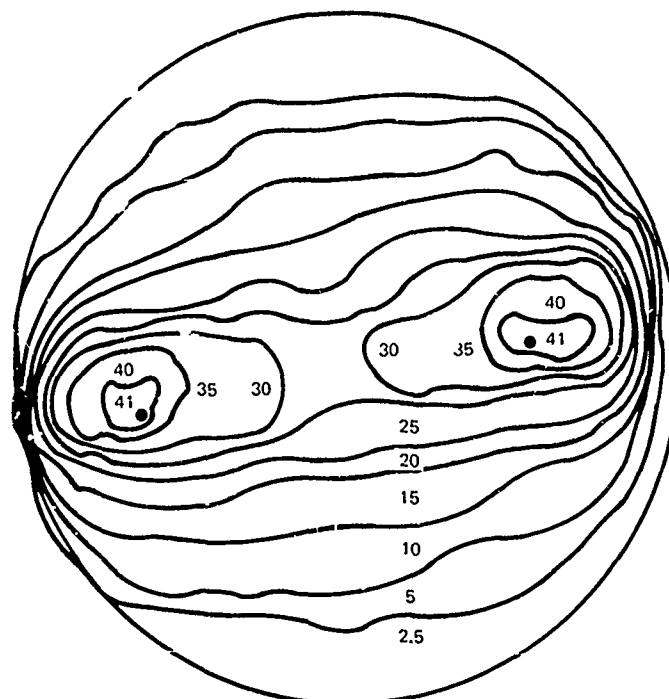
A 0.5-mm thickness quartz, cylindrical glass insert was painted with 6080 Eastman White Reflectance Paint and installed in a cylindrical pump cavity. This paint is a composition of barium sulfate, binder, and solvent specially prepared to form coatings with reflectance higher than magnesium oxide throughout the ultraviolet, visible, and part of the near-IR region of the spectrum. It has nearly perfect diffuse reflection properties. Figure 8 shows a representative PPD distribution for a diffusely reflecting cylindrical pump cavity configuration. The beam uniformity parameter $M^* = 2.75$ for this case. The reduction in M^* as compared to the silvered cylindrical pump cavity with inserts is attributed of course to the improved pumping uniformity of the laser rod. When using the diffusely reflecting pump cavity, the output energy was near 25% less than when using the cylindrical pump cavity with inserts (the same end reflector was used in each case). The M^* value is relatively independent of pump power (and so, laser output) as will be shown shortly.



$$M^* = 2.75$$

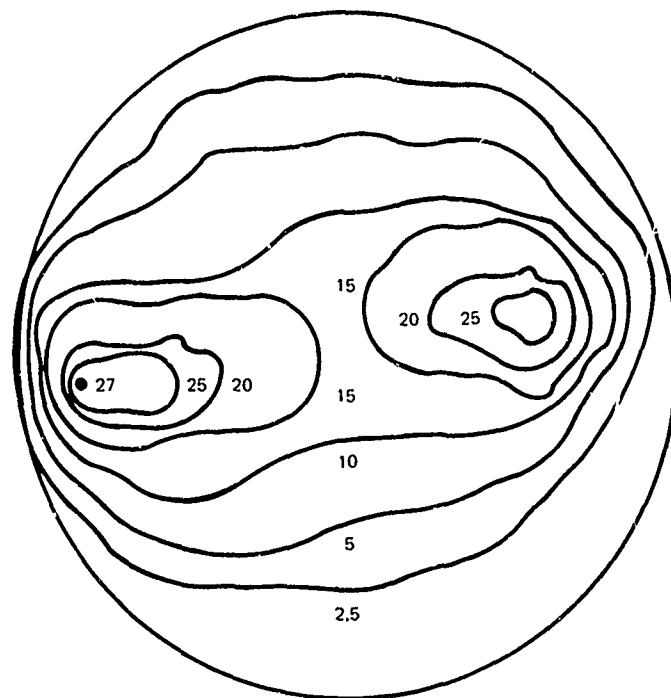
FIG. 8. Peak Power Density Distribution for a Diffusely Reflecting Cylindrical Pump Cavity Geometry.

Figure 9 shows a representative PPD distribution profile near the resonator output aperture for the silvered close-wrapped pump cavity configuration. (As in earlier contour profile diagrams, the krypton-filled flashlamp was located to the left of the contour diagram.) The parameter $M^* = 3.06$ for this case and averaged $M^* = 3.06$ as well. The "hot spot" at the right of the contour diagram is attributed to the focusing property of the close-wrapped configuration (which has semi-circular ends of 0.165-inch radius). As in prior M^* measurements, the pump level was 8 joules per pulse. The PPD distribution obviously remains relatively unchanged for an input pump level of only 6 joules as seen in Fig. 10.



$M^* = 3.06$

FIG. 9. Peak Power Density Distribution for the Close-Wrapped Pump Cavity, 8-Joule Input.



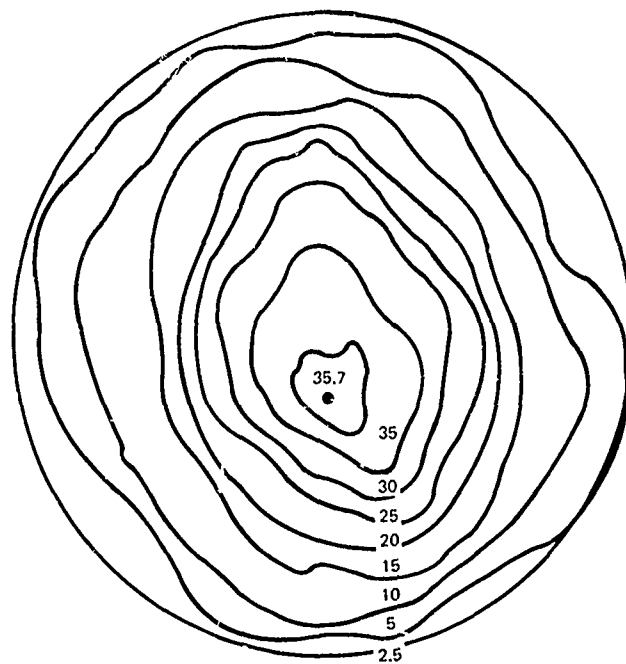
$$M^* = 2.97$$

FIG. 10. Peak Power Density Distribution for the Close-Wrapped Pump Cavity, 6-Joule Input.

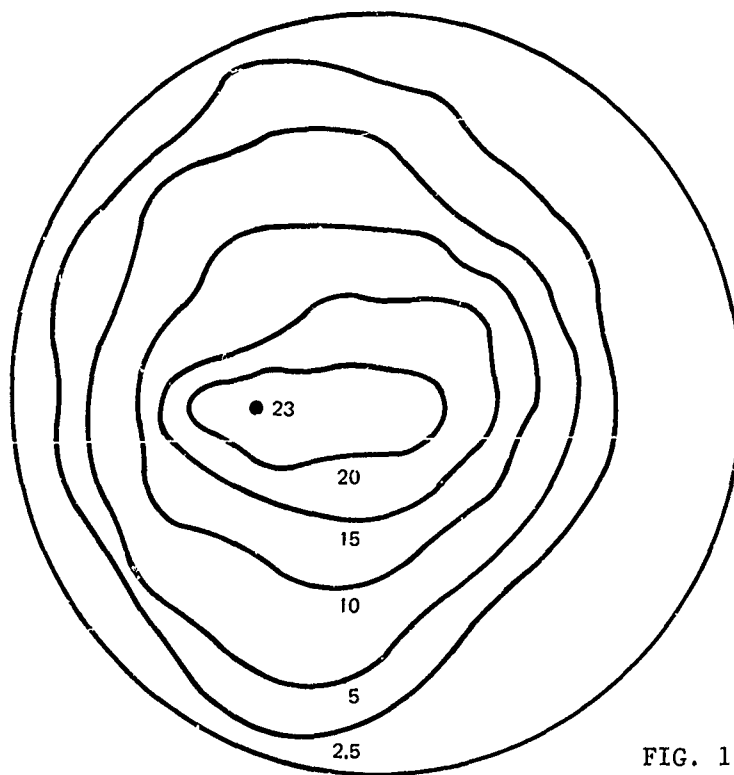
Figure 11 shows a representative PPD distribution contour mapping for the silvered cylindrical pump cavity configuration. The pump cavity coupling parameter $M^* = 3.08$ for this case, whereas the average M^* value for all measurements made on this pump cavity coupling configuration had $M^* = 3.13$.

The effect on M^* of a misaligned laser resonator is also of interest. A laser resonator may become misaligned due to environmental conditions, stress effects, etc., or, as is the case with FC-104 coolant, a thermal misalignment of the resonator may occur. To produce the equivalent misalignment condition, the 100% end mirror was misaligned slightly shifting the PPD distribution in the laser rod. The energy output reduction with respect to the aligned resonator case was about 10%. Figure 12 shows the PPD distribution for a typical misaligned resonator using a silvered cylindrical pump cavity shape, and has $M^* = 3.25$.

FIG. 11. Peak Power Density Distribution for a Silvered Cylindrical Pump Cavity Shape.



$M^* = 3.08$



$M^* = 3.25$

FIG. 12. Peak Power Density Distribution for a Representative Misaligned Laser Resonator.

The distribution in output energy for a non-Q-switched laser resonator is shown in Fig. 13. It is apparent that a considerable redistribution of energy has occurred relative to the Q-switched case. The M^* figure for this case was not calculated. The output energy distribution for this case is perhaps more representative of the distribution of absorbed flashlamp radiation by the laser rod. Prior laboratory measurements on the non-Q-switched resonator using a motor-driven scanning aperture show that the output beam uniformity is more dependent upon the end reflector used as compared to the Q-switched case.

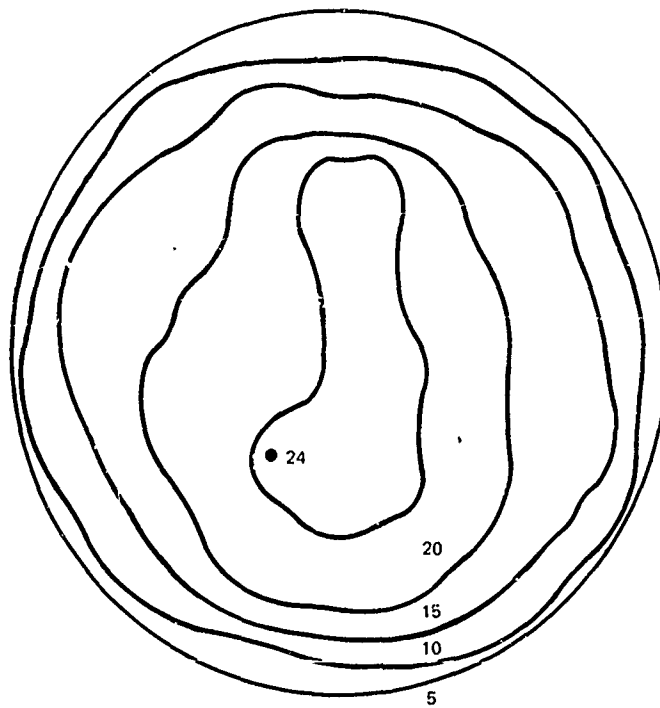


FIG. 13. Energy Contour Mapping for a Non-Q-Switched Laser Resonator.

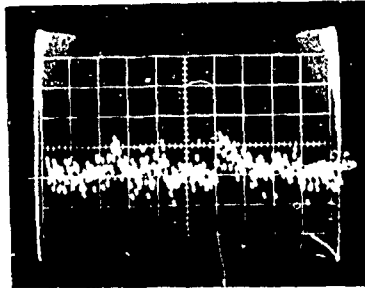
ENERGY OUTPUT STABILITY

The Q-switched pulse-to-pulse and long-term energy output stability of the laser was excellent. The EG&G radiometer was used to make energy output stability measurements six times (for a 10-sec interval) during a 10-min laser run time, i.e., about the time required to complete one data matrix. The pulse-to-pulse and long-term energy output variation was less than 3% over this run time, except for a brief laser warm-up time. Recall that the past M^* measurements have used an integrated signal output at a Sanborn recorder. The scan aperture was placed at or near the position of maximum PPD where the energy output stability is expected to be the worst. Figure 14(a) shows this "hot spot" energy output stability soon after the laser was turned on, and indicates that the equilibrium thermal conditions in the laser rod were not yet well established. However, the pulse-to-pulse energy output stability recorded at the photodiode (when positioned at this most intense beam position) is greatly improved after about 1 minute of laser operation as shown in Fig. 14(b). (These photographs were taken using a 50-ohm load at the scope input.) The signal voltage was negative and the lowest position of the trace is proportional to the PPD being sensed per pulse. The output stability at the photodiode was improved slightly when the scan aperture was moved from near the maximum PPD position. Since the pulse-to-pulse and long-term laser output stability, both at the radiometer and at the scan aperture, was excellent (after a short warm-up time), no experimental details of the beam uniformity measurements are lost by signal integration. The signal voltage integration improved the recorder signal stability slightly by averaging the $\mu A740$ output and its inherent noise due to the high fields generated by flashlamp triggering, modulator drive, and energy storage capacitor discharge through the flashlamp.

HOT SPOT SIZING

For the four pump cavity coupling configurations tested, the average M^* value then varied from $M^* = 2.75$ for the diffusely reflecting cylindrical pump cavity shape to $M^* = 3.86$ for the silvered cylinder pump cavity with inserts. This means that, in small regions on the lithium niobate modulator (as elsewhere within the resonator), the maximum PPD is from 220-300 MW/cm^2 when the average intra-resonator PPD is only 80 MW/cm^2 . Hence, it appears that the small region of maximum PPD is where surface damage on the modulator is most likely to occur. A sizing of the "hot spot" near the maximum PPD position was made to provide data on its size relative to the typical damage spot size commonly observed on lithium niobate modulators. By moving the scan aperture in 0.005-inch increments in both the horizontal and vertical plane, the "hot spot"

size diagram of Fig. 15 was derived. The contour line encloses the area where the PPD is, rather arbitrarily, within 5% of the maximum PPD figure recorded. This enclosed area is approximated by a circle of 0.017-inch diameter.



(a) Time base, 5 sec/div;
amplitude, 2 V/div; output
stability at warm-up.

(b) Time base, 5 sec/div;
amplitude, 1 V/div; output
stability after 2 min of
run time.

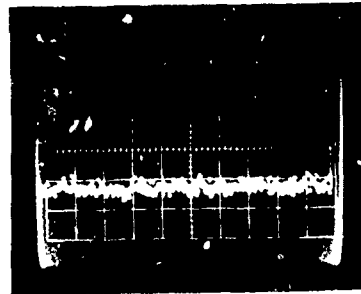
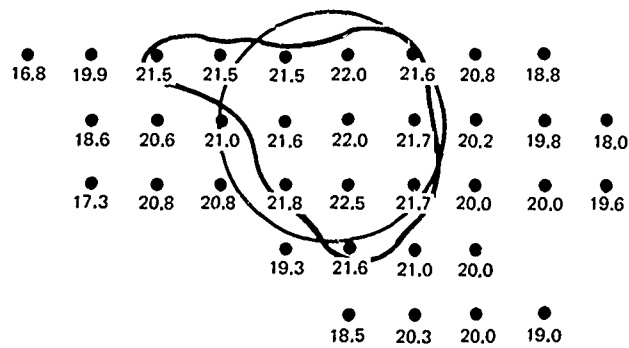


FIG. 14. "Hot Spot" Output Stability.



MATRIX ELEMENT SPACING: 0.005 IN.

FIG. 15. "Hot Spot" Sizing Data Matrix.

The 9- x 9- x 10-mm lithium niobate modulator was examined under 100X magnification using a Nomarski phase contrast microscope. The surface imperfections were mapped out in an approximate way prior to exposure to the Q-switched laser radiation when used actively as the Q-switch. Both surfaces of the modulator had minute areas where no anti-reflecting (AR) coating was present. The non-AR-coated areas were roughly circular in shape and varied in diameter. It appeared that the multilayer, dielectric AR coating was once applied to these areas (judging by the jagged appearance of the edges of such areas), but, for some reason, did not adhere. No difference was seen in the surface quality of the lithium niobate between the non-AR-coated and the properly AR-coated areas. After several days of use as a Q-switch, slight damage was noted on one surface of the modulator. The following observations were made regarding this damage (using 500X magnification):

1. There were five damage spots within an area of about 0.012 x 0.035 inch near the center of one face of the crystal.
2. The two major damage spots were located on sites where surface imperfections were noted prior to exposure to Q-switched laser radiation.
3. The major damage sites were approximately 0.002 x 0.010 inch and 0.002 x 0.005 inch in size. The surface AR-coating imperfections as observed prior to Q-switched radiation exposure were of approximately the same dimensions as well.
4. The three secondary damage sites may have occurred at less obvious surface imperfections since many more minor non-AR-coated areas were present than were noted in the prior modulator examination. They may also have occurred as a result of the molten ejecta spewn from the two major damage sites (craters) noted earlier.
5. All of the damage sites were of nearly equal depth.
6. Very much smaller damage sites were present near the center faces of the modulator. These damage sites were nearly circular in shape and less than 0.002 inch in diameter.

It is most significant that most of the surface damage occurred in an area on the lithium niobate modulator where unusually high PPD was accompanied by a surface imperfection. It is also noteworthy that the damage sites were much smaller than the lowest order mode diameter. Since the surface damage diameter observed on lithium niobate was much smaller than the measured "hot spot" diameter of 0.017 inch, the modulator microscopic imperfections (either on its surface or internal) or a focusing effect (as may be due to an induced index of refraction gradient) must be contributing to the surface damage threshold level.

FAR FIELD BEAM UNIFORMITY

The data matrix elements and a representative PPD distribution in the far field for a diffusely reflecting cylindrical pump cavity are shown in Fig. 16. The matrix elements are separated in angle increments of 0.617 mrad as explained earlier. Using the discrete point-averaging technique, it follows that $M^* = 2.67$ and, within 10%, the M^* value in the far field is equal to the M^* value near the resonator output aperture. Hence the maximum PPD is about 2.7 times larger than the average PPD, regardless of whether M^* is measured near the resonator or in the focal plane of a lens. Note that the peak signal level is shifted slightly toward the flashlamp side of the laser rod.

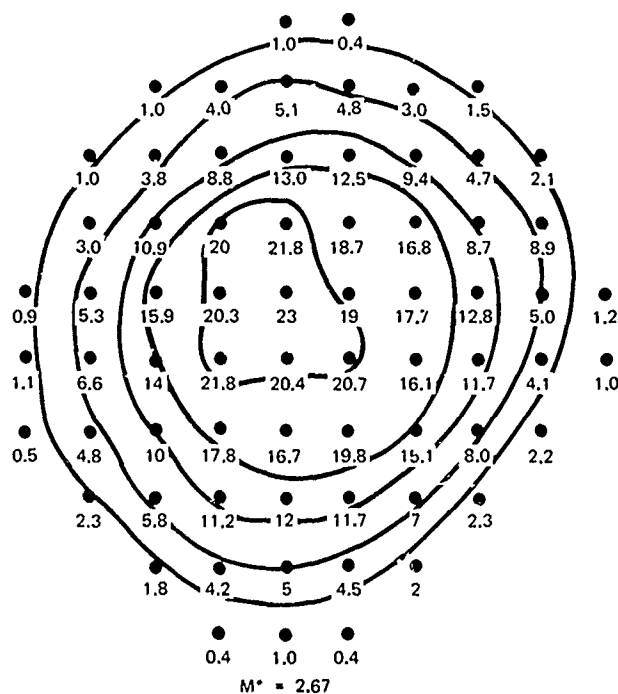


FIG. 16. Far Field Peak Power Density Distribution for a Diffuse Cylindrical Pump Cavity Shape.

A data matrix and a representative far field PPD distribution for a close-wrapped pump cavity configuration are shown in Fig. 17. Obviously the PPD distribution is far from Gaussian in nature. This close-wrapped pump cavity configuration obviously provides two "hot spots," both of which are near the edge of the laser output beam. An aim error that may prevent all but a fractional part of the beam from striking a target may still contain an appreciable percentage of the output energy of the laser. The beam uniformity parameter $M^* = 3.3$ for this case, which is within 10% of the average M^* value measured near the resonator output aperture as well.

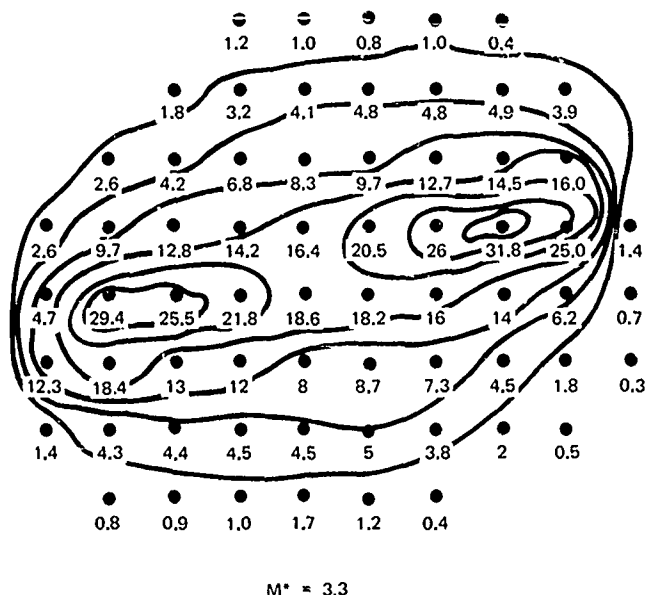


FIG. 17. Far Field Peak Power Density Distribution for a Close-Wrapped Pump Cavity Shape.

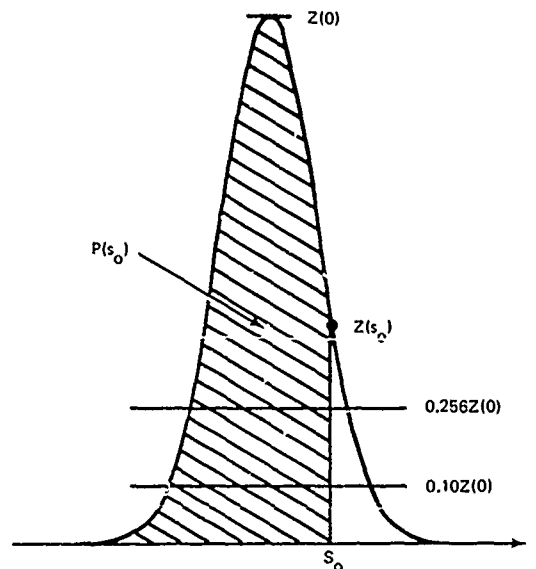
These two pump cavity configurations provided an M^* value and a PPD distribution in the far field similar to that recorded near the resonator output aperture. Though not shown here, the cylindrical pump cavity with inserts had a far field beam uniformity very similar to that shown in Fig. 7(a). The parameter $M^* = 2.75$ for this case. The silvered cylindrical pump cavity was not tested in the far field, since, by the prior measurements, the M^* value was independent of where the measurement was made.

BEAM DIVERGENCE MEASUREMENTS

Some laser manufacturers measure raw beam divergence by scanning with a small aperture in the focal plane of a very long focal length lens. On the basis of the present far field beam uniformity tests, this scanning aperture approach to the measurement of beam divergence can be compared quantitatively to the more common technique of measuring energy content by using apertures of various sizes in a lens (or mirror) focal plane.

Figure 18 shows the pertinent variables and their dependence for a (norm. 1) Gaussian distribution. The table of Fig. 18 shows that, for a Gaussian distribution, 96.8% of the output energy lies within the points

0.10 of peak amplitude $Z(0)$ and 90% of the output energy (momentarily considering energy content as the percentage of the area under the normal Gaussian curve) lies within $Z(s)$ equal to 25.6% of the peak amplitude $Z(0)$, i.e., $0.256 Z(0)$. Note that the difference in s -value, which is directly proportional to beam divergence, is a factor of 0.77. Actually a measurement of energy content through an aperture requires that the normal Gaussian be considered two-dimensionally. For this case it can be shown mathematically that the beam divergence measurement techniques, for a true Gaussian, should yield identical results. In actual fact, however, it will be shown that the difference in beam divergence for the two measurement techniques is roughly a factor of 0.77 for the particular pump cavity tested. (This is attributed to the fact that the beam intensity distribution is not truly two-dimensionally Gaussian.) The scanning aperture approach requires that the output beam profile be scanned at its widest position in the focal plane of the positive lens and is more subject to measurement errors than is the fixed-aperture approach.



THE VARIABLES

- $P(s_0)$ = NORMALIZED AREA UNDER THE GAUSSIAN CURVE TO THE LEFT OF s_0
- $Z(s_0)$ = AMPLITUDE OF POSITION s_0

WHERE

- (a) $P(-s) = 1 - P(s)$
- (b) $Z(s) = (2\pi)^{-1/2} e^{-s^2/2}$
- (c) $Z(s) = Z(-s)$
- (d) $P(s) = \int_{-\infty}^{-s} Z(t) dt$

DESCRIPTION	AMPLITUDE	ENERGY CONTENT	s
10% POINTS OF PEAK AMPLITUDE	$Z(0)/10$	96.8%	2.146
90% POINTS OF ENERGY CONTENT	$0.256 Z(0)$	90.0%	1.650

FIG. 18. Gaussian Distribution Variables.

Circles have been drawn on the peak power density distribution of Fig. 19 which should correspond to the 2.3, 5, 10, 15, and 20 unit contours, assuming that the energy output distribution is truly Gaussian and that the outermost contour line corresponds to $Z(0)/10$. Evidently the agreement to a Gaussian distribution is only approximate. The data used to draw these equivalent Gaussian contours is given in Table 1. The aperture diameter D is the aperture size required in the lens focal plane to pass the laser energy whose signal amplitude is larger than the corresponding amplitude $Z(s)$. Hence, the raw beam divergence--using the signal amplitude $Z(0)/10$ (i.e., the 10% points of peak amplitude) to establish the aperture diameter D required--is given by the ratio $D/(\text{lens focal length}) = 5.0 \text{ mrad}$. A fixed aperture measurement (passing 90% of total laser output energy) of beam divergence should yield, then, a beam divergence of $(5.0)(0.77) = 3.8 \text{ mrad}$. This value is in excellent agreement with experimental results. This beam divergence figure (at a fixed input pump power) has been shown to be relatively insensitive to the pump cavity shape in those cases where the output beam distribution has a similarity to a Gaussian distribution.

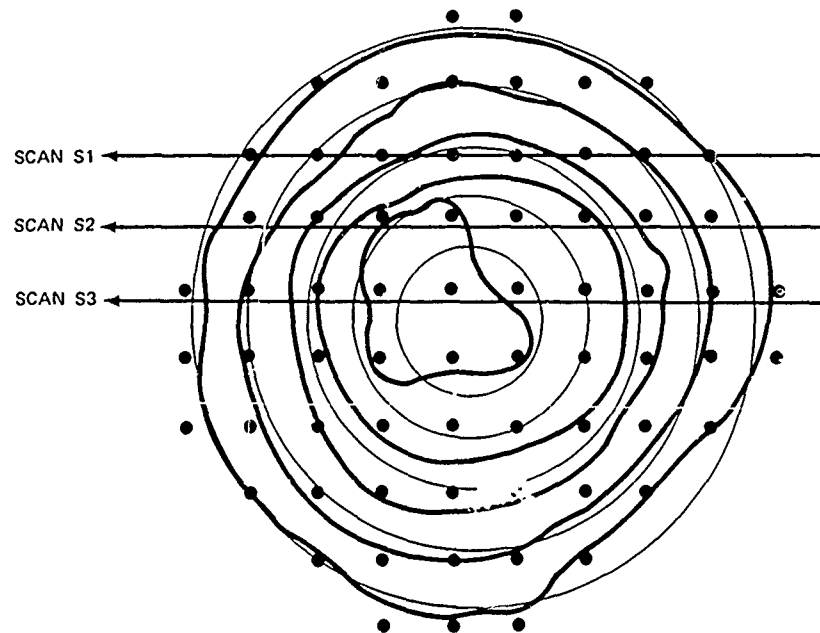


FIG. 19. Actual Peak Power Density to Gaussian Distribution Comparison for Diffuse Pump Cavity Shape.

TABLE 1. Gaussian Contour Plotting Data.

Contour ident.	Amplitude Z(s)	s	Scale factor	Aperture diam. D, in.
2.3	0.10 Z(0)	2.15	86	0.206
5.0	0.22 Z(0)	1.74	70	0.168
10.0	0.44 Z(0)	1.28	51	0.122
15.0	0.65 Z(0)	0.93	37	0.089
20.0	0.87 Z(0)	0.53	21	0.050

The actual energy output distribution for the diffuse cylindrical pump cavity shape deviates from the Gaussian distribution as can be seen from the motor-driven aperture scan profiles of Fig. 20. The horizontal scan positions S1, S2, and S3 and the direction of aperture travel are shown in Fig. 19. The scan profile has a steeper slope on the flashlamp side of the laser rod. So, although the output energy distribution is not ideally Gaussian, even for the diffusely reflecting cylindrical pump cavity shape, the 10% peak amplitude measurement (using a scanning aperture approach) and 90% energy content measurement (the fixed aperture approach) of beam divergence are equivalent when the appropriate weighting factor of 0.77 is applied.

The silvered close-wrapped pump cavity shape provides an output beam uniformity that is extremely non-Gaussian. For such a pump cavity shape no correlation of beam divergence measurement technique (scanning aperture versus fixed aperture) is possible. It is noteworthy, however, that a measurement of beam divergence using the fixed aperture approach (to include 90% of the laser output energy) would require an aperture size nearly as large as the beam spot major diameter (namely, about 6 mrad--as seen by Fig. 17), since appreciable energy is contained near the beam edge. If a scanning aperture approach were used, the beam divergence would measure approximately 6 mrad (horizontally) by 3.1 mrad (vertically).

LASING AREA AND AN M* DATA SUMMARY

The M* data presented assumes the lasing area A is an invariant for the various pump cavity coupling configurations tested. A planimetric measurement of a PPD contour whose amplitude is equal to 10% of the peak amplitude reveals that the enclosed area for Fig. 7 through 10 and Fig. 12 is, at the least, 0.268 cm² (Fig. 12) and, at the most, 0.284 cm² (Fig. 7 and 9)--a difference of only 5%. Hence, within an accuracy of $\pm 2.5\%$, the lasing area is a constant. The average lasing area for all the PPD distributions presented was 0.279 cm².

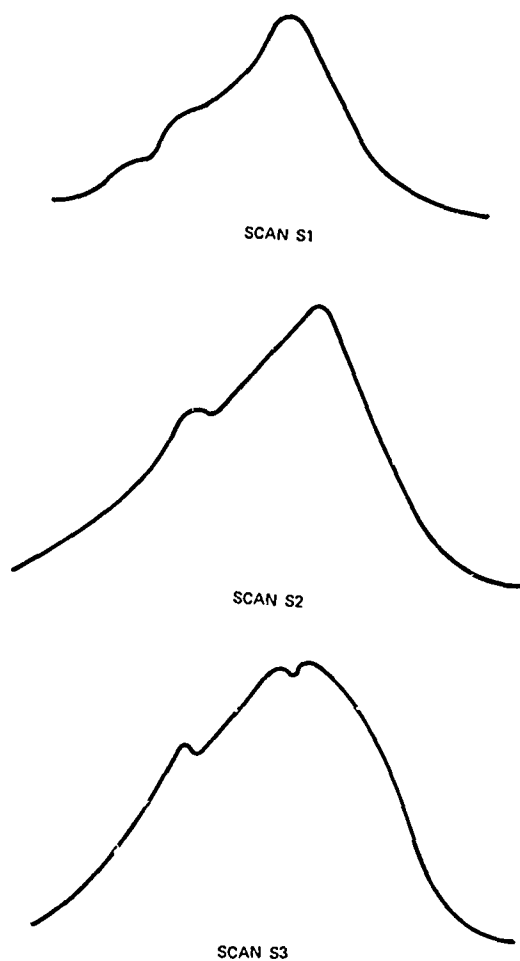


FIG. 20. Scan Profiles in Far Field.

Table 2 provides an M^* data summary for the various pump cavity configurations tested. It provides the average M^* values, the accuracy of the measurement, and some of the test conditions. Unless otherwise noted, the input energy was 8 joules per pulse at a 10-Hz rate. Evidently the M^* value for a particular pump cavity is relatively independent of the resonator reflector used (flat or 10-meter), the input energy level (over the rather narrow range tested), the alignment quality of the resonator (10% output reduction), or where the M^* measurement is made (near the resonator output aperture or in the focal plane of a positive lens). The M^* parameter is more akin to a pump cavity coupling (uniformity) parameter than simply a beam uniformity parameter.

TABLE 2. M* Data Summary

Cavity ident.	M*	End mirror	Av. M*	Av. error, %	RMS error, %	Comments
Silvered cyl.	2.8	10-m	3.13	4.85	3.8	Fig. 11
	3.08	10-m				
	3.12	flat				
	3.25	10-m				
	3.42	10-m				
Silvered cyl. with inserts	3.6	10-m	3.86	2.85	2.0	Far field case Fig. 7(a)
	3.75	flat				
	3.82	flat				
	3.87	10-m				
	3.90	10-m				
	4.0	10-m				
	4.05	10-m				
Diffuse cyl.	2.67	10-m	2.71			Far field case, Fig. 16 Fig. 3
	2.75	10-m				
Silvered close-wrapped	2.96	10-m	3.06	2.94	1.5	Fig. 10 Fig. 9 Far field case, Fig. 17
	2.97	10-m				
	3.03	10-m				
	3.06	10-m				
	3.3	10-m				

The silvered cylindrical pump cavity has an M* value only 20% larger than that of the diffusely reflecting cylindrical pump cavity. Tests have shown that the latter pump cavity has a lasing efficiency approximately 20% less than the silvered cylindrical pump cavity shape. The data summary of Table 2 also indicates that, if maximum PPD is a potential problem within the resonator, the silvered cylindrical pump cavity with inserts should not be used, since it has an M* figure nearly 20% larger than the silvered cylindrical pump cavity tested. The close-wrapped pump cavity has a beam uniformity distribution that makes it unacceptable for use in some Nd:YAG laser applications.

CONCLUSION

The beam uniformity parameter M^* ("M-Star") was measured and tabulated for four flashlamp-laser rod pump cavity coupling configurations. It was shown that the factor M^* , the ratio of the maximum PPD to the average PPD, varies from $M^* = 2.67$ for a diffuse cylindrical pump cavity configuration to $M^* = 3.86$ for a silvered cylindrical pump cavity with inserts. As a result, the ratio of PPDs would be nearly 2:3 for the above pump cavities, even though their energy output and beam divergence figure may be similar.

The silvered cylindrical pump cavity with inserts, due to its large M^* value, should not be used in those resonators where the energy output is dictated by PPD considerations. In turn, the silvered cylindrical pump cavity had $M^* = 3.13$, only about 15% larger than the M^* value for the diffusely reflecting cylindrical pump cavity shape. The silvered cylindrical pump cavity shape was the most efficient coupling geometry tested as well.

The scanning aperture and fixed aperture approaches for measuring beam divergence were shown to be equivalent for a Gaussian beam distribution when the appropriate weighting factor was applied. The silvered close-wrapped cavity tested was shown to have an extremely non-Gaussian beam distribution, which generally increases the output beam divergence and makes such a pump cavity shape unacceptable for use in some laser applications.

The test procedure and data reduction technique (discrete point-averaging) were described and can be used to determine M^* for other coupling geometries, e.g., silvered elliptical. The data on M^* values for the coupling configurations tested applies only to those described here and should not be extended to similar pump cavity shapes with different physical dimensions.

The M^* value was shown to be applicable toward improving the pump cavity design, improving our understanding of missile and seeker tracking behavior, and as an aid in establishing the actual damage threshold level to retinal tissues as well as laser resonator components.

Distribution List
Not Filmed

Page 28

UNCLASSIFIED

Security Classification

DOCUMENT CONTROL DATA - R & D		
<i>Security classification of title, body of abstract and indexing annotation must be entered when the overall report is classified</i>		
1. ORIGINATING ACTIVITY (Corporate author) Naval Weapons Center China Lake, Calif. 93555		2a. REPORT SECURITY CLASSIFICATION UNCLASSIFIED
		2b. GROUP
3. REPORT TITLE BEAM UNIFORMITY MEASUREMENTS FOR Q-SWITCHED Nd:YAG LASERS		
4. DESCRIPTIVE NOTES (Type of report and inclusive dates)		
5. AUTHOR(S) (First name, middle initial, last name) Edward A. Teppo		
6. REPORT DATE February 1972	7a. TOTAL NO. OF PAGES 28	7b. NO. OF REFS
8a. CONTRACT OR GRANT NO.	9a. ORIGINATOR'S REPORT NUMBER(S) NWC TP 5315	
b. PROJECT NO.		
c.	9b. OTHER REPORT NO(S) (Any other numbers that may be assigned this report)	
d.		
10. DISTRIBUTION STATEMENT Distribution limited to U.S. government agencies only; test and evaluation; 15 February 1972. Other requests for this document must be referred to the Naval Weapons Center.		
11. SUPPLEMENTARY NOTES	12. SPONSORING MILITARY ACTIVITY Naval Air Systems Command Washington, D.C. 20360	
13. ABSTRACT <p>The output beam uniformity of a Q-switched Nd:YAG laser, using four different flashlamp-laser rod pump cavity coupling configurations, is described. The test apparatus and test procedure used to establish the beam uniformity quantitatively are given.</p> <p>A newly defined beam uniformity parameter M^*, the ratio of maximum-to-average peak power density, is shown to vary significantly for the pump cavities tested. The data presented on beam uniformity is applicable toward improving laser pump cavity design, interpreting particular missile and seeker tracking behavior, comparing techniques for measuring laser beam divergence and is an aid in establishing the damage threshold level for retinal tissues and laser resonator components at 1.06 μ.</p>		

DD FORM 1473 (PAGE 1)

1 NOV 65
S/N 0101-807-6801

UNCLASSIFIED
Security Classification

14

KEY WORDS

LINK A

LINK B

LINK C

ROLE

WT

ROLE

WT

ROLE

WT

Beam uniformity
Pump cavity comparison
Q-switched Nd:YAG laser
Beam divergence
Laser safety

ABSTRACT CARD

Naval Weapons Center

Beam Uniformity Measurements for Q-Switched Nd:YAG Lasers, by Edward A. Teppo. China Lake, Calif., NWC, February 1972. 28 pp. (NWC TP 5315, publication UNCLASSIFIED.)

The output beam uniformity of a Q-switched Nd:YAG laser, using four different flashlamp-laser rod pump cavity coupling configurations, is described. The test apparatus and test procedure used to establish the beam uniformity quantitatively are given.

A newly defined beam uniformity parameter M^* , the ratio of maximum-to-average peak power density, is

(Over)

1 card, 8 copies



Naval Weapons Center

Beam Uniformity Measurements for Q-Switched Nd:YAG Lasers, by Edward A. Teppo. China Lake, Calif., NWC, February 1972. 28 pp. (NWC TP 5315, publication UNCLASSIFIED.)

The output beam uniformity of a Q-switched Nd:YAG laser, using four different flashlamp-laser rod pump cavity coupling configurations, is described. The test apparatus and test procedure used to establish the beam uniformity quantitatively are given.

A newly defined beam uniformity parameter M^* , the ratio of maximum-to-average peak power density, is

(Over)

1 card, 8 copies



Naval Weapons Center

Beam Uniformity Measurements for Q-Switched Nd:YAG Lasers, by Edward A. Teppo. China Lake, Calif., NWC, February 1972. 28 pp. (NWC TP 5315, publication UNCLASSIFIED.)

The output beam uniformity of a Q-switched Nd:YAG laser, using four different flashlamp-laser rod pump cavity coupling configurations, is described. The test apparatus and test procedure used to establish the beam uniformity quantitatively are given.

A newly defined beam uniformity parameter M^* , the ratio of maximum-to-average peak power density, is

(Over)

1 card, 8 copies



Naval Weapons Center

Beam Uniformity Measurements for Q-Switched Nd:YAG Lasers, by Edward A. Teppo. China Lake, Calif., NWC, February 1972. 28 pp. (NWC TP 5315, publication UNCLASSIFIED.)

The output beam uniformity of a Q-switched Nd:YAG laser, using four different flashlamp-laser rod pump cavity coupling configurations, is described. The test apparatus and test procedure used to establish the beam uniformity quantitatively are given.

A newly defined beam uniformity parameter M^* , the ratio of maximum-to-average peak power density, is

(Over)

1 card, 8 copies



NWC TP 5315

shown to vary significantly for the pump cavities tested. The data presented on beam uniformity is applicable toward improving laser pump cavity design, interpreting particular missile and seeker tracking behavior, comparing techniques for measuring laser beam divergence and is an aid in establishing the damage threshold level for retinal tissues and laser resonator components at 1.06 μ .

NWC TP 5315

shown to vary significantly for the pump cavities tested. The data presented on beam uniformity is applicable toward improving laser pump cavity design, interpreting particular missile and seeker tracking behavior, comparing techniques for measuring laser beam divergence and is an aid in establishing the damage threshold level for retinal tissues and laser resonator components at 1.06 μ .

NWC TP 5315

shown to vary significantly for the pump cavities tested. The data presented on beam uniformity is applicable toward improving laser pump cavity design, interpreting particular missile and seeker tracking behavior, comparing techniques for measuring laser beam divergence and is an aid in establishing the damage threshold level for retinal tissues and laser resonator components at 1.06 μ .

NWC TP 5315

shown to vary significantly for the pump cavities tested. The data presented on beam uniformity is applicable toward improving laser pump cavity design, interpreting particular missile and seeker tracking behavior, comparing techniques for measuring laser beam divergence and is an aid in establishing the damage threshold level for retinal tissues and laser resonator components at 1.06 μ .